GEOLOGICA CARPATHICA, 2026, 77, 5, 391–406 https://doi.org/10.31577/GeolCarp.2026.20

Autolith enclaves in Pan-African Ediacaran peralkaline granite from the Abu Kharif area, Eastern Desert of Egypt: Insights from mineral chemistry

NASSER MOURAD MAHDY[1,2,✉]

[1]Nuclear Materials Authority, P.O. 530, El-Maadi, Cairo, Egypt
[2]Department of Mineralogy, Petrology and Economic Geology, Faculty of Natural Sciences, Comenius University, Mlynská dolina, Ilkovičova 6, 84215 Bratislava, Slovakia

(Manuscript received May 4, 2026; accepted in revised form August 20, 2026; Associate Editor: Igor Broska)

Abstract: The Abu Kharif peralkaline granite (AKPG) with Ediacaran age in the Eastern Desert of Egypt, as a part of the Arabian–Nubian Shield (ANS), hosts abundant finer-grained microgranular enclaves (MEs). Such MEs are rare in peralkaline A-type granites, and their origin remains poorly constrained. The Abu Kharif MEs and host granite share similar mineral assemblages, including albite ($Ab_{99}An_1$), K-feldspar ($Or_{97}Ab_3$), ferroan Na–Ca amphibole (mostly ferro-richterite, katophorite, and ferro-winchite), Mn-rich ilmenite (up to 12.8 wt.% of MnO), quartz, and Ti-rich magnetite (up to 15.6 wt.% of TiO_2), but differ in modal proportions. Titanite occurs exclusively in the enclaves and is interpreted to be hydrothermal in origin, where it replaces amphibole. Furthermore, Mn-rich ilmenite, Ti-rich magnetite, and zircon are more abundant in the host granite, while quartz is less abundant in the enclaves. Overall, the MEs are rich in mafic minerals – particularly amphibole, titanite, and ilmenite – comprising >50 vol.% of the mode, which is inconsistent with a liquid composition. Their field, mineralogical, and textural characteristics instead support a cogenetic origin, consistent with autolithic model. The finer grain size of the MEs reflects crystallization under undercooling conditions, likely at magma chamber margins during the emplacement, while their ellipsoidal shapes and mineralogical similarity to the host granite indicate plastic behavior and thermal equilibrium. These features suggest that the MEs represent accumulations of early-formed mafic minerals, i.e., autoliths. Ferro-richterites from the Abu Kharif MEs are more magnesian than those in the host granite and together define coherent compositional trends – characterized by positive correlations of Al with Ca and Ti and negative correlations with Si and Na – indicating a progressive magma differentiation. These well-defined chemical linear trends observed in amphiboles further support a cogenetic origin of the host AKPG and its MEs within a shared magmatic evolution.

Keywords: A-type granite, microgranular enclaves, Na–Ca amphiboles, genetic model, Arabian–Nubian Shield, cognate cumulate

Introduction

The MEs are compositionally, texturally, and genetically distinct fragment, globule, or crystal-rich aggregate enclosed within a host igneous rock, preserving evidence of petrogenetic processes such as magma injection, magma mingling and incomplete mixing, assimilation of country rock, fractional crystallization, crystal accumulation, and magma chamber replenishment during the evolution of the host magma. The most common genetic models, that have been proposed for the origin of MEs, include: (i) the xenolith model (e.g., Kumar et al. 2004; Zafar et al. 2020); (ii) the restite model (e.g., Chen et al. 1989); (iii) the autolith (cognate cumulate) model (e.g., Blundy & Sparks 1992; Perugini et al. 2004); and (iv) magma mingling and mixing processes (e.g., Kumar & Rino 2006; Kumar & Pieru 2010; Barnes et al. 2021; Eliwa et al. 2021).

Xenoliths are foreign lithic fragments, typically derived from country rock and incorporated during the magma emplacement (e.g., Vernon 1983). In contrast, restites are interpreted as refractory residues of the source material that failed to attain a critical melt fraction during the partial melting (e.g., Chappell & White 1991). Some enclaves "autoliths" represent accumulations of early formed, genetically related crystals entrained within their own residual melt (e.g., Schönenberger et al. 2006; Shellnutt et al. 2010), whereas others reflect magma mixing and mingling between compositionally distinct magmas, typically involving injection of hotter mafic magma into cooler felsic magma. Mixing produces a homogeneous hybrid melt, whereas mingling preserves compositional contrasts, commonly as MEs (e.g., Eliwa et al. 2021).

Although enclave genetic models are commonly presented as distinct mechanisms, they are better regarded as end-member processes that may operate sequentially or simultaneously during the evolution of granitoid magmatic systems. Several recent studies demonstrate that many enclaves preserve evidence of multiple petrogenetic processes (Chen et al. 2018; Wu et al. 2020; Gómez-Frutos & Castro 2023; Domańska-

✉ corresponding author: Nasser Mourad Mahdy
nassermahdy91@yahoo.com
omar9@uniba.sk

Siuda et al. 2024). For example, a restitic fragment inherited from the source region may be incorporated into an ascending felsic magma and subsequently undergo partial melting, chemical exchange, recrystallization, and hybridization, thereby obscuring its primary characteristics (Domańska-Siuda et al. 2024). Similarly, cognate enclaves representing early crystallized portions of the host magma may later interact with replenishing magma batches, while xenolithic fragments may be thermally and chemically modified through partial assimilation and recrystallization, producing overlapping petrographic and geochemical characteristics. Therefore, enclave types should be viewed as representing a continuum of interconnected magmatic processes rather than mutually exclusive genetic categories.

Although the MEs are abundant and widely documented in I- and S-type granitoids (e.g., Perumalsamy et al. 2024), they are comparatively uncommon in peralkaline A-type granites due to the distinctive petrogenetic evolution of A-type magmatic systems, in which highly evolved, alkali-rich magmas, lower magma viscosities, prolonged fractional crystallization, and efficient chemical homogenization may reduce the preservation of discrete MEs (e.g., Barbarin 1999; Shellnutt et al. 2010), despite several well-documented examples demonstrating that they can form where mafic and felsic magmas interact during the evolution of A-type magmatic systems (Kontonikas-Charos et al. 2023; Domańska-Siuda et al. 2024). Therefore, their study in the peralkaline granitic magma provides valuable insights into this uncommon phenomenon. The mineral chemistry and textural characteristics of the Abu Kharif peralkaline granite (AKPG) and its enclaves (Egypt) can offer an opportunity to constrain the origin of microgranular enclaves in peralkaline, silica-saturated A-type granitoids and their implications for the magmatic evolution.

Geological setting and sample description

The Pan-African Orogeny (~950–550 Ma) and the Variscan orogeny (~380–280 Ma) represent major tectonothermal events, with the latter extensively reworking crust formed from the former. The Variscan Orogeny reflects a large-scale Late Paleozoic collision between Gondwana and Laurussia, culminating in the assembly of Pangaea and the emplacement of extensive granitic batholiths across Europe (e.g., Stampfli & Borel 2002; Fréville et al. 2024). These granitoids formed through widespread crustal anatexis associated with subduction, continental collision, and subsequent orogenic collapse, as documented in Variscan granitic systems of the Western Carpathians (e.g., Petrík & Broska 1994; Kohút & Larionov 2021; Broska et al. 2022; Spišiak et al. 2024; Kohút et al. 2024). A substantial proportion of these magmas was generated by reworking Ediacaran–Ordovician Gondwanan basement (e.g., Mandl et al. 2022), with petrogenetic evidence indicating derivation mainly from partial melting of felsic meta-sedimentary and meta-igneous protoliths within the continental crust, originally part of the passive margin (Putiš et al. 2024; Broska et al. 2024a).

The East African Orogen (EAO) records a major Neoproterozoic orogenic system formed during the closure of the Mozambique Ocean and represents a key component in the assembly of Gondwana lands (e.g., Jacobs & Thomas 2004). Its northern continuation is exposed as the Arabian–Nubian Shield (ANS), which provides an exceptional record of juvenile crustal growth in northeast Africa and Arabia. The EAO basement reflects a pronounced north–south contrast, with high-grade metamorphic complexes of the Mozambique Belt in the south and predominantly low-grade metamorphic units of volcanic, plutonic, and sedimentary origins to the north (Cox et al. 2012). The ANS formed during the EAO (ca. 950–550 Ma), following the breakup of Rodinia (Stern 1994), and records a prolonged history of crustal accretion, arc magmatism, and tectonic amalgamation throughout the Cryogenian and Ediacaran periods.

The major lithotectonic units of the ANS in the Eastern Desert and Sinia Peninsula of Egypt can be summarized from the oldest to the youngest (Stern 2018; Mahdy et al. 2024) as follows: (1) High-grade gneisses, amphibolites, and migmatites form core complexes. (2) Dismembered ophiolites (780–730 Ma) are represented by serpentinite, ophiolitic gabbros, and ophiolitic pillow basalts (Kröner et al. 1994). (3) Arc assemblage and arc-volcanic clastic metasediments (780–620 Ma) are represented by older metavolcanics (called ophiolitic arc related), metasediments (greenschist facies volcaniclastic wackes/pelites and diamictite along with occasional banded iron formation; El-Shazly & Khalil 2016), and metagabrrodiorite complexes (island-arc calc-alkaline gabbro–diorite complexes). (4) Hammamat molasse-type sediments (600–585 Ma) and Dokhan volcanics (620–550 Ma).

Granitoid magmatism of the ANS in Egypt is commonly subdivided into two major phases, locally referred to as older and younger granitoids (El-Bialy et al. 2020). The older granitoids are syn-tectonic (ca. 670–590 Ma), subduction-related, calc-alkaline magmas with I-type affinity, spanning compositions from quartz diorite to monzogranite. In contrast, the younger granitoids are predominantly post-tectonic (ca. 590–550 Ma) and reflect more evolved magmatic conditions associated with late- to post-collisional tectonics. These granitoids range from calc-alkaline to alkaline characteristics and include highly fractionated I-type and A-type granites. Within this framework, the AKPG (identified before as alkali riebeckite granite; Abdel Wanees et al. 2022) represents a late-stage, Ediacaran anorogenic alkaline magmatism (Zircon U–Pb age of 614.6±3.6 Ma ; Dessouky et al. 2024).

The Abu Kharif area is located in the Northern Eastern Desert of Egypt between 33°21’–33°28’ E and 26°47’–26°50’ N (Fig. 1) and is about 60 km away from Safaga-City, Red Sea governate. The exposed lithological succession comprises metavolcanics, gneissose granodiorite, W-rich biotite granite (Mahdy 2026), and peralkaline granite (current study) (Fig. 1b). The metavolcanics represent the oldest units and consist mainly of metarhyolite, metadacite, and metabasalt, locally

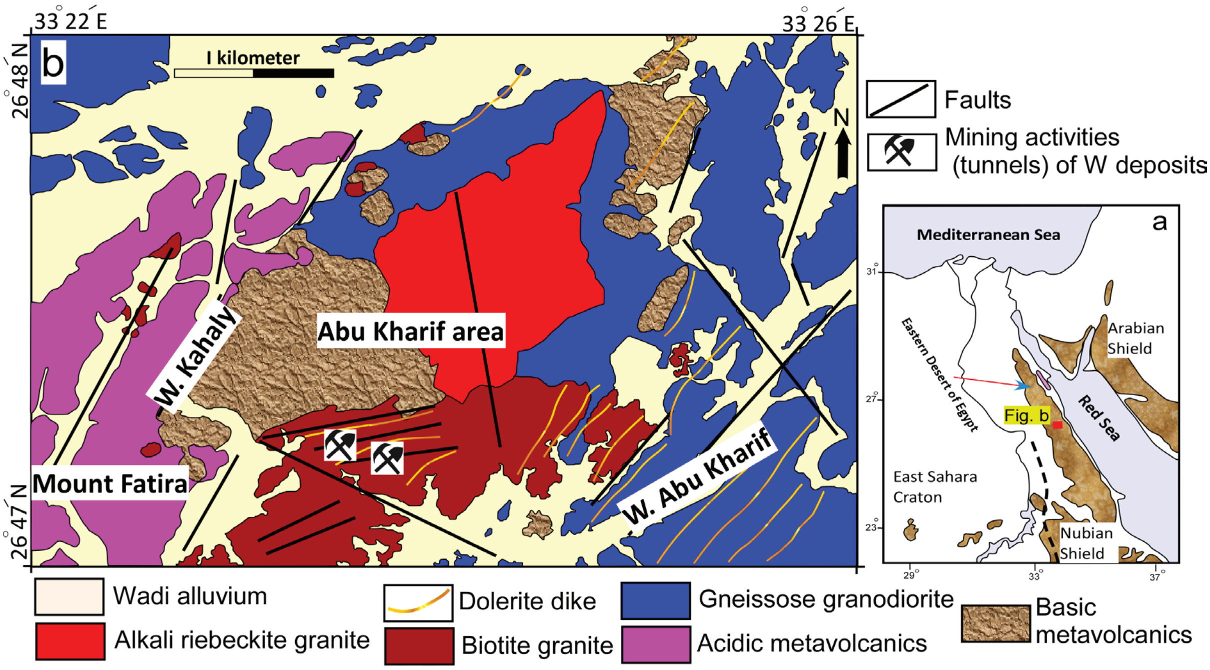

Fig. 1. (a) Geological map of Egypt showing the location of the study area within the Arabian–Nubian Shield (brown-shaded region). **(b)** Geological map of the Abu Kharif area illustrating the location of the peralkaline granite hosting microgranular enclaves and associated country rocks, modified after Abdel Wanees et al. (2022) and Mahdy (2026).

associated with interbeds and lenses of metapyroclastic rocks. These rocks show colour variations and distinct metamorphic features, while the metabasalt is weakly foliated and locally shows greenschist-facies metamorphism. The metavolcanics are intruded by granitoid rocks, including gneissose granodiorite and W-rich biotite granite, which are subsequently crosscut by the AKPG (Fig. 2). Most units, except the latter, are transected by dolerite dykes and quartz veins.

The AKPG is classified as an A_1-type anorogenic granite (El-Sayed 1998; Abdel-Rahman 2006; Abdel Wanees et al. 2022). It forms rugged, mountainous ridges and is characterized by a leucocratic appearance, medium- to coarse-grained texture, and pink to reddish coloration. The granite exhibits sharp intrusive contacts with the surrounding country rocks and represents the youngest lithological unit in the study area, as it is not crosscut by any dykes or veins. Whole-rock geochemical data (see Abdel Wanees et al. 2022 for analytical details) indicate that the host granite is characterized by high SiO_2 (average 77.26 wt.%), total alkalis (Na_2O+K_2O; average 8.35 wt.%), and total iron (FeO_{total}; average 2.13 wt.%), together with relatively low Al_2O_3 (average 11.25 wt.%) and very low P_2O_5 (average 0.01 wt.%). The agpaitic index (AI=(Na+K)/Al; Liégeois & Black 1987) averages 1.10, confirming the peralkaline affinity of the granite. Primitive mantle-normalized multi-element patterns exhibit pronounced negative anomalies in Sr, P, and Ti, together with moderate depletion in Ba, consistent with extensive feldspar and Fe–Ti oxide fractionation (Bonin 2007; Frost & Frost 2011). The granite is further characterized by low Y/Nb ratios (<1.2), corresponding to the A1-type granite classification of Eby (1992). Moreover, the low Y/Nb (average 0.99) and Yb/Ta (average 2.00) ratios indicate limited crustal contamination during magma evolution, as significant crustal assimilation typically increases these trace-element ratios (Eby 1992; Wilson 2007).

The MEs within the AKPG are abundant and widely distributed throughout the pluton. They vary in size and shape, typically ranging from 2 to 6 cm in diameter. The enclaves are microgranular and fine- to medium-grained, with predominantly elongate to oval or rounded shapes rather than angular forms (Fig. 2). They are readily distinguished from the host granite by their darker coloration; however, this contrast primarily reflects differences in modal mineralogy rather than sharp physical boundaries. Although the colour contrast may suggest well-defined contact, the enclaves commonly exhibit diffuse boundaries with the host granite, lacking any contact aureole or reaction fronts. Moreover, many mineral phases are shared between the MEs and the host AKPG. In the hand specimen, it is worthy notable that the enclaves have higher abundance of amphibole and other mafic minerals, and correspondingly less quartz compared to the host granite. In addition, large K-feldspar phenocrysts are conspicuous within the enclaves (Fig. 2).

Methodology

Due to their small size (mainly 3 cm), the abundance of K-feldspar megacrysts, and their diffuse contact with the host AKPG, it is difficult to obtain uncontaminated samples of MEs. Consequently, any whole-rock geochemical data may be

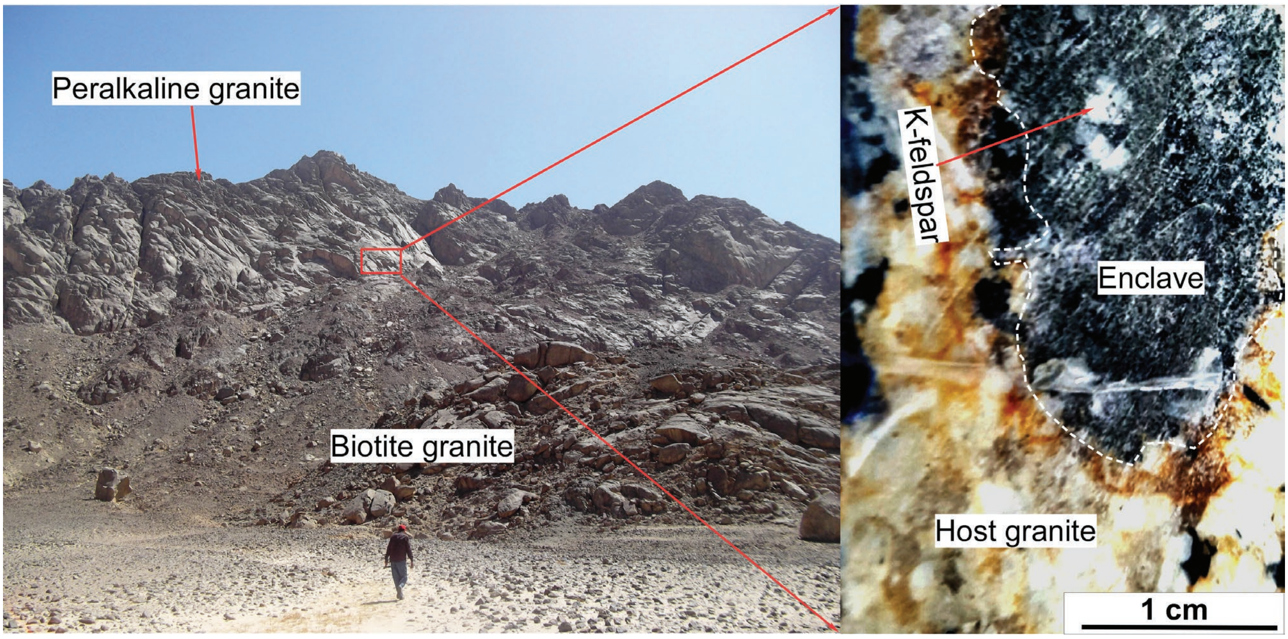

Fig. 2. Field and hand specimen photographs illustrating: **(a)** the peralkaline granite intruding the older biotite granite and its characteristic smooth morphology; **(b)** hand specimen showing darker microgranular enclaves with diffuse contacts against the host granite. Note that the enclaves contain inclusions of K-feldspar megacrysts.

unrepresentative. Therefore, this study has a focus on petrography, mineralogy, and mineral chemistry to investigate the mineral textural and chemical characteristics of both the host AKPG and the MEs, as well as to constrain their genetic relationships.

Optical polarizing microscope and back-scattered electron (BSE) imaging

Seventeen standardized (30 µm) polished thin sections of the AKPG and MEs were prepared for petrographic and mineralogical studies using an optical polarizing microscope at the Nuclear Materials Authority of Egypt. A subset was selected for mineral imaging and chemical analysis and then coated with carbon. Prior to mineral chemistry measurements, BSE images were used to examine the internal zoning structures of minerals, determine whether inclusions or alterations were present, and analytical spot selection. The BSE images were obtained using a JEOL JSM-7000F Field Emission Scanning Electron Microscope at the Department of Earth and Planetary Science, The University of Tokyo, Japan. The operating conditions used an accelerating voltage of 10 kV, an emission current of 20 nA, and a working distance of 10 mm.

Electron probe microanalyses (EPMA)

The chemical composition of K-feldspar, plagioclase, amphibole, and accessory minerals was determined by a Field Emission-EPMA JEOL JXA 8530F HyperProbe at The University of Tokyo, Japan. The operating conditions of Electron Probe Microanalysis (EPMA) included a beam diameter of 2 µm, a probe current of 30 nA, and an accelerating voltage of 15 kV. Peak count and background times for major elements were 10 s and 5 s, respectively, whereas for trace elements they were 30 s and 15 s. Natural and synthetic standards were used for calibration and the ZAF matrix correction was then applied to the raw data. To assess elemental distributions within the minerals of the host peralkaline granite and associated enclaves at the granite-enclave boundary, X-ray elemental mapping was performed on the majority of felsic and mafic minerals with the following operating conditions: an acceleration voltage and beam current of 25 kV and 30 nA, respectively, and a beam mode of a circle with a diameter of 1–2 um.

Petrography and BSE imaging

The AKPG exhibits an equigranular texture (Fig. 3) and is composed predominantly of K-feldspar (54 vol.%) and quartz (27 vol.%), with minor plagioclase (10 vol.%). Amphiboles constitute ~9 vol.% of the peralkaline granite and are represented by ferroan to potassian sodic–calcic amphiboles, which were identified by electron probe microanalysis as ferro-richterite (50 vol.% of the total amphibole amount), katophorite (25 vol.%), and ferro-winchite (25 vol.%). Accessory minerals include mainly zircon and Fe–Ti oxides (Mn-rich ilmenite and Ti-rich magnetite). Potash feldspar crystals occur as coarse- to medium-grained subhedral, reaching up to 7 mm in length and 4 mm in width. These crystals are present in two forms: perthite and antiperthite. Potash feldspar crystals display various perthitic textures, including flame-, vein-, feather-, and patch-like exsolution lamellae (Fig. 3a), as well as cross-hatched

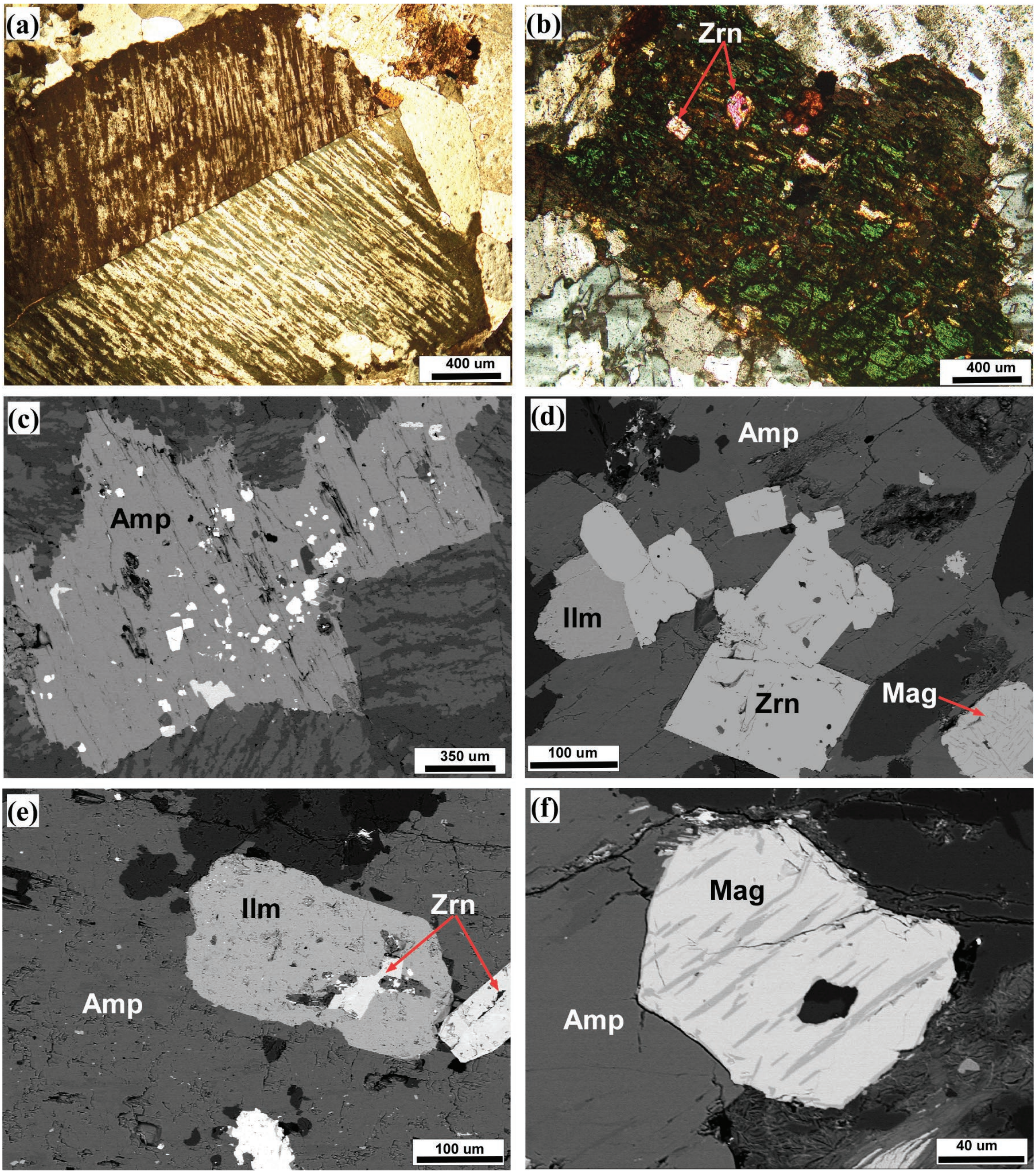

Fig. 3. Optical photomicrographs and back-scattered electron (BSE) images of the host peralkaline granite showing: **(a)** feather-like perthite; **(b, c)** large amphibole crystal enclosing zircon and other mineral inclusions; **(d)** cluster of bipyramidal zircon associated with anhedral ilmenite and titanomagnetite as inclusions in amphibole; **(e)** euhedral ilmenite containing inclusions of fine zircon crystals; and **(f)** well-formed Ti-rich magnetite included in amphibole. Mineral abbreviations: Zrn=zircon; Amp=amphibole; Ilm=ilmenite; Mag=magnetite.

microcline twinning. Plagioclase occurs as subhedral to anhedral crystals with prismatic form and is commonly associated with K-feldspars, exhibiting albitic twinning. Quartz commonly occurs as coarse-grained, anhedral crystals with oval to globular shapes, filling the interstitial spaces between K-feldspar crystals. Amphiboles are coarse-grained (up to 5 mm in size), euhedral to subhedral, prismatic in habit, and show strongly pleochroic (Fig. 3b, c). Some amphibole crystals occur as acicular aggregates or as interstitial phases between K-feldspar crystals. Zircon and Fe–Ti oxides commonly occur as inclusions within amphiboles and K-feldspar crystals (Fig. 3d–f). Zircon (mainly 50–350 µm in size) occurs in bipyramidal short prismatic crystals (Fig. 3d). Ilmenite forms anhedral to euhedral elongated crystals, ranging from 60 to 500 µm in size (Fig. 3e), whereas Ti-rich magnetite typically occurs as euhedral crystals, ranging from 50 to 300 µm in size (Fig. 3f). These accessories are frequently found in intimate association with one another, often as inclusions in amphiboles.

The Abu Kharif enclaves are fine-grained and composed predominantly of amphiboles, titanite, K-feldspars, and albite, with accessory minerals of quartz and Fe–Ti oxides (Fig. 4). Most of the mineral phases occur as anhedral crystals and commonly appear as intergrowths or interstitial phases rather than well-formed individual crystals. Potash feldspar constitutes approximately 40 % of the modal composition and typically occurs as perthitic grains that are rectangular, equant, or subrounded in shape. Abundant K-feldspar megacrysts display well-developed crystal forms and pronounced perthitic textures, typically ranging from 2 to 4 mm in size (Fig. 4a–c). These megacrysts exhibit irregular, undulating boundaries against the surrounding fine-grained matrix and commonly contain inclusions of amphibole, titanite, and other finer-grained silicates. Amphiboles, predominantly ferrorichterite with minor ferrowinchite, are the most abundant mafic minerals in the enclaves, comprising ~40 % of the modal composition (Fig. 4c–f). The crystals are typically fine-grained and range from anhedral to subhedral in habit. Most amphibole grains occur interstitially between feldspars or host inclusions of finer-grained, anhedral to equant crystals of feldspars (Fig. 4d, e) and Fe–Ti oxides. Titanite is fine-grained and typically occurs as anhedral crystals, comprising approximately 15 % of the modal composition. It commonly contains inclusions of Fe–Ti oxides, predominantly magnetite, and occurs in association with amphiboles. Textural relationships indicate that titanite frequently develops at the expense of amphibole, displaying clear hydrothermal replacement textures (Fig. 4f). These include irregular reaction boundaries, embayed amphibole relics, and partial to complete pseudomorphic replacement. Accessory minerals include fine-grained, equant to anhedral Mn-rich ilmenite and other Fe–Ti oxide minerals, along with quartz occurring as anhedral to subhedral grains. Most of these accessories occur as inclusions within, or interstitial to, amphibole and K-feldspar crystals (Fig. 4c–f).

Mineral chemistry and X-ray elemental maps

Feldspars: The major element compositions of K-feldspar and plagioclase in the AKPG and associated MEs, as determined by electron probe microanalyses (EPMA), are presented in Supplementary Tables S1 and S2, respectively. Potassium feldspars from both the host AKPG and MEs exhibit similar compositions, averaging $Or_{97.3}Ab_{2.7}$ and $Or_{96.6}Ab_{3.4}$, respectively, and plot within the perthitic microcline field on the Or–Ab–An ternary diagram (Fig. 5a). Plagioclase compositions are typically pure albite (Fig. 5a) and are also comparable between the AKPG and MEs, averaging $Ab_{99.3}An_{0.7}$ and $Ab_{99.1}An_{0.9}$, respectively.

Amphiboles: EPMA analyses of amphiboles from the host AKPG and MEs are presented in Supplementary Table S3. Amphiboles from the host AKPG and MEs exhibit similar compositions and are classified as sodic–calcic (Fig. 5b) according to the nomenclature of Hawthorne et al. (2012). They are characterized by high Fe contents, ranging from 4.67 to 4.33 apfu in the host granite and from 4.40 to 4.26 apfu in the enclaves. Sodium contents are also high, with values of 1.51–1.22 apfu in the host granite and 1.54–1.28 apfu in the enclaves. The $Mg/(Mg+Fe^{2+})$ ratios are generally low but variable in the host granite (0.09–0.02), whereas they are relatively restricted in the enclaves (0.10–0.08). Based on the classification scheme of Leake et al. (1997), amphibole compositions from the host AKPG plot within the fields of ferro-richterite, katophorite, and ferro-winchite, while those from the MEs fall within the ferro-richterite and ferro-winchite fields (Fig. 5c, d).

Accessory minerals: Ilmenite was analyzed in the host granite and enclaves, titanite only in enclaves, and Ti-rich magnetite only in the host granite, according to their relative abundances in the respective units. Major element compositions of **ilmenite** are listed in Supplementary Table S4. Ilmenite in both the host AKPG and related MEs shows similar compositions, with TiO_2 (46.71–53.92 wt.% and 50.84–52.78 wt.%, respectively), FeO (33.92–46.32 wt.% and 35.87–44.94 wt.%), and variegated MnO (0.15–12.76 wt.% and 3.25–10.20 wt.%) contents. Aluminum, Si, and Na are below detection limits. Based on the classification scheme of Mitchell & Liferovich (2004), chemical analyses are classified as Mn-rich ilmenite (Fig. 5e). EPMA data and calculated structural formulae for **titanite** are presented in Supplementary Table S5. Structural formulae are calculated based on three cations, assuming that all iron is incorporated into the crystal lattice as Fe^{3+} (King et al. 2013). Titanite displays a restricted compositional range in SiO_2 (28.5–29.6 wt.%; 0.95–1.02 apfu Si) and CaO (23.99–26.57 wt.%; 0.88–0.96 apfu Ca) but exhibits more variable TiO_2 contents (32.76–38.71 wt.%; 0.85–0.98 apfu Ti). On the Fe vs. Al (apfu) diagram, the analyses plot outside the igneous field, suggesting a hydrothermal origin (Fig. 5f). The Fe/Al ratios are notably high, ranging from 3.87 to 10.6, most likely consistent with the replacement for ferroan Na–Ca amphiboles in the MEs. The major-element compositions of **magnetite** in the host AKPG are presented in Supplementary Table S6. This oxide mineral is dominated by Ti-rich magnetite, with TiO_2 contents reaching up to 15.6 wt.% (0.27 apfu Ti). The predominance of Ti-rich magnetite suggests crystallization under moderately oxidizing conditions, typical of evolved alkaline magmatic systems.

Elemental distribution maps for Ca, Fe, K, Mn, Al, Ti, and Si, together with BSE image and composite element map, are presented in Figure 6. These elemental maps focus on the

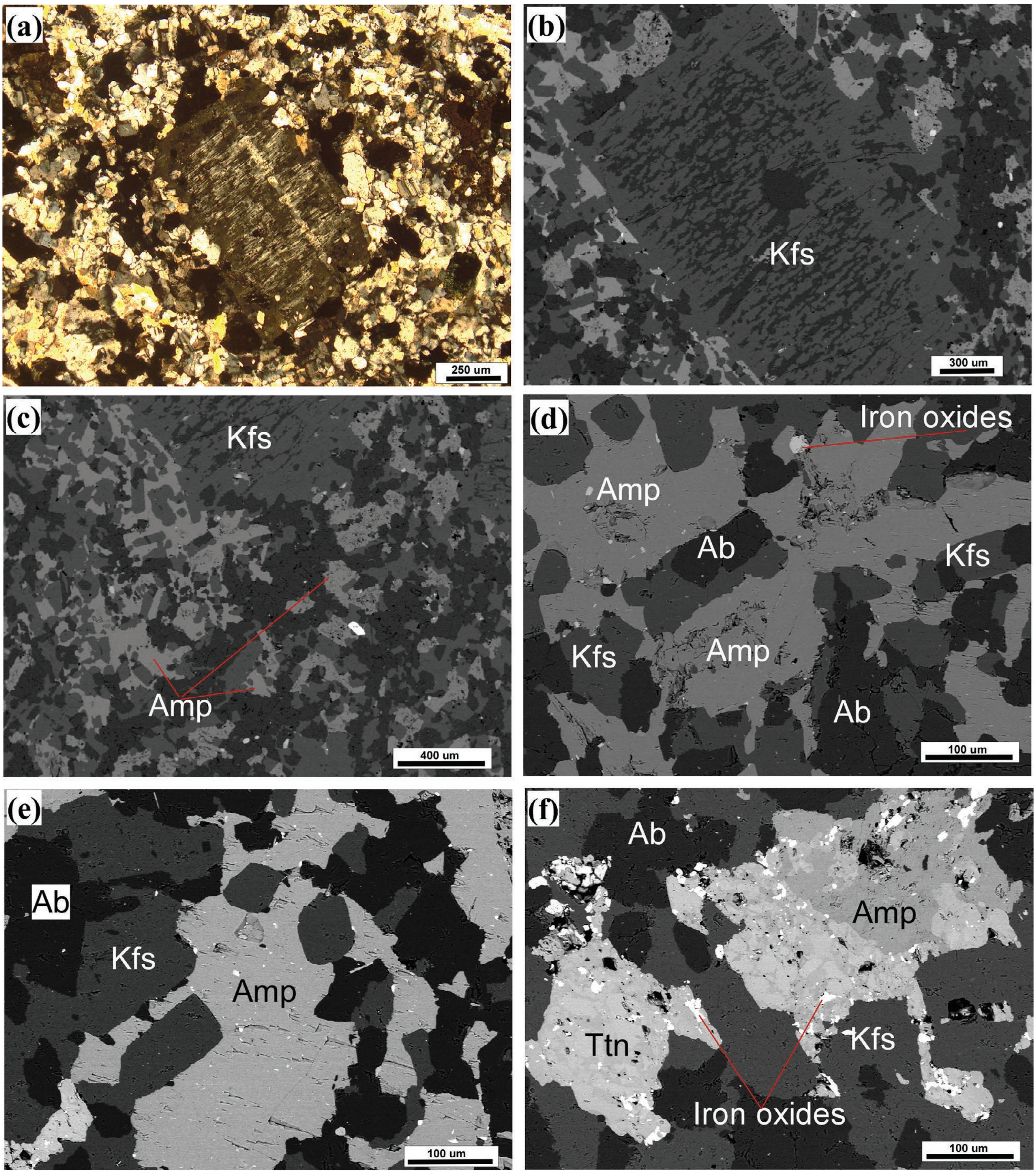

Fig. 4. Optical photomicrographs and BSE images of the microgranular enclaves showing: **(a, b)** large K-feldspar crystals surrounded by fine-grained mafic minerals; **(c)** representative BSE image showing the textural characteristics of the enclaves associated with K-feldspar megacrysts. The enclaves are predominantly composed of feldspars and amphiboles, defining the principal mineral assemblage and enclave–host textural relationships; **(d, e)** anhedral crystals of amphibole associated with feldspars and containing fine, equant K-feldspar inclusions; and **(f)** anhedral crystals of titanite after amphiboles. Mineral abbreviations: Kfs=K-feldspar; Ab=albite; Tnt=titanite; other abbreviations as in Fig. 3.

dominant mineral phases at the interface between the host AKPG and MEs. The elemental distributions highlight the prevalence of titanite replacing amphibole within the enclaves, as well as the dominance of ferroan Na–Ca amphiboles, whereas the host granite is characterized by quartz and feldspar-rich assemblages. These compositional contrasts are accompanied by diffuse contact along the enclave–granite boundary. Furthermore, the elemental maps emphasize the

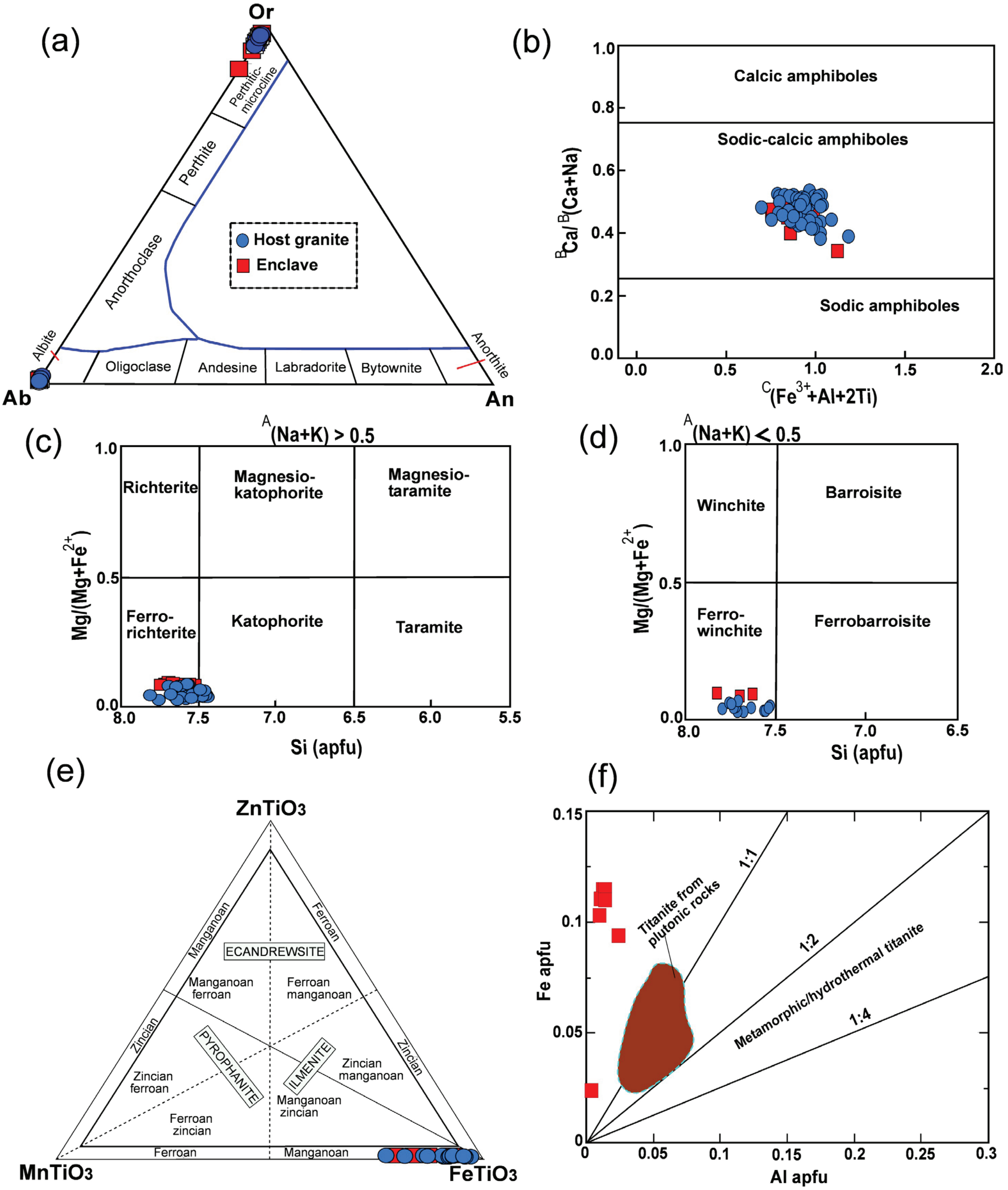

Fig. 5. Chemical classification diagrams for common mineral phases in the host peralkaline granite and its enclaves: **(a)** Or–Ab–An ternary diagram for feldspars; **(b)** amphibole classification based on the nomenclature of Hawthorne et al. (2012); **(c, d)** amphibole classification diagrams following the scheme of Leake et al. (1997); **(e)** nomenclature and classification of the Abu Kharif Mn-bearing ilmenites in triangular diagram with three end members $ZnTiO_3$–$FeTiO_3$– $MnTiO_3$ after Mitchell & Liferovich (2004); and (**f**) Fe (apfu) versus Al (apfu) diagram for titanite (Kowallis et al. 2022), showing compositions inconsistent with typical plutonic titanite.

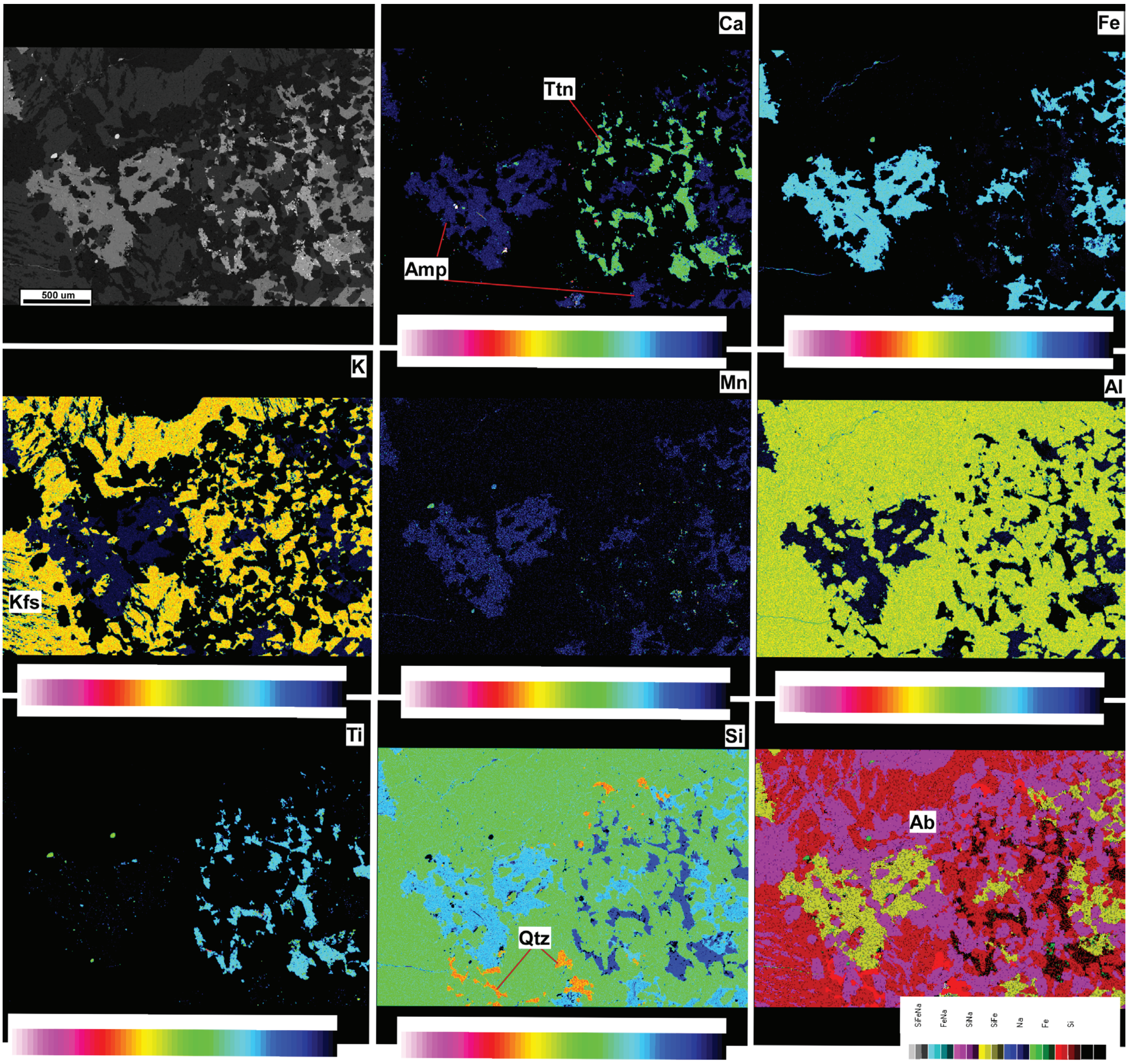

Fig. 6. Elemental distribution maps for Ca, Fe, K, Mn, Al, Ti, and Si, together with BSE image and composite element map, illustrating the interface between the host peralkaline granite and its enclave. Mineral abbreviations: Qtz=quartz; Ab=albite; other abbreviations as in Figs. 3 and 4.

mineralogical continuity between the enclaves and their host, reinforcing the interpretation that both units share a common magmatic origin.

Discussion

Evaluation of proposed genetic models

The xenolith and restite models are considered unlikely for the origin of the MEs in the AKPG, as evidenced by the absence of contact aureoles, metamorphic fabrics, and cross-cutting relationships with the host granites. In the restite model, MEs are interpreted as residual or unmelted fragments of meta-sedimentary or meta-igneous source rocks preserved after partial melting during granite magma generation (e.g., White et al. 1999). Based on whole-rock geochemical data (Abdel Wanees et al. 2022), the AKPG was derived from partial melting of metasomatized Pan-African granitic crust. Its REE pattern closely resembles that of a calculated melt produced by ~65 % non-modal batch melting of metasomatized Pan-African calc-alkaline granites. However, the Abu Kharif MEs lack metamorphic fabrics, reaction or resorption textures, and refractory minerals (such as zircon) inherited from their metasomatized calc-alkaline granitoids source. Instead, they exhibit a simple mineral assemblage dominated by amphibole and feldspars, largely overlapping with that of the host granite (Fig. 4). The AKPG is characterized by high Zr concentrations (472–686 ppm), consistent with its peralkaline affinity (Abdel Wanees et al. 2022). The occurrence of zircon aggregates enclosed within sodic calcic amphiboles of the AKPG is characteristic of evolved peralkaline granites. This association reflects the high solubility of Zr in alkali- and volatile-rich peralkaline melts, which delays zircon saturation until the late stages of magmatic differentiation (e.g., Boehnke et al. 2013). As the residual melt becomes enriched in Zr through fractional crystallization, zircon crystallizes contemporaneously with late-stage alkali amphiboles and is entrapped during their growth (Marks & Markl 2017; Salvi & Williams-Jones 2022). Furthermore, the fine-grained igneous microstructures (Fig. 6) of the MEs (Vernon 2010) are inconsistent with a restite origin.

In addition, the MEs commonly display elliptical to rounded shapes, and locally diffuse contacts with the host AKPG (Fig. 2), indicating that they behaved as ductile to plastic bodies during the emplacement. These features suggest mechanical and thermal equilibration with the host granitic magma rather than a solid-state incorporation. The absence of chilled margins or thermal overprinting further argues against a xenolithic origin. Moreover, the mineralogical compositions (mafic minerals > 50 %) and textural characteristics of the Abu Kharif MEs (Figs. 4 and 6) differ markedly from those of the surrounding country rocks (gneissose granodiorites, metagabbro–diorite complexes, and metavolcanics), precluding derivation from local wall-rock fragments. Geochemically, the AKPG is characterized by low Y/Nb (average 0.99) and Yb/Ta (average 2.00) ratios (Abdel Wanees et al. 2022), which are inconsistent with significant crustal contamination or assimilation (Wilson 2007). These chemical signatures argue against substantial interaction with the country rocks through partial assimilation or xenolith entrainment.

Diagnostic mixing–quench textures – such as quartz ocelli, cellular and resorbed plagioclase, elongate amphibole, and acicular phases – typically produced by rapid cooling and mechanical interaction between coexisting distinct magmas (i.e., hotter mafic and relatively cooler felsic magmas; e.g., Petrík & Broska 1994; Eliwa et al. 2021), are absent in the Abu Kharif MEs. This lack of textural evidence argues against magma mixing or mingling processes. Moreover, mafic–felsic magma interaction (including mixing, mingling, and undercooling) is commonly invoked to explain the origin of the MEs in I-type granites (e.g., Broska et al. 2013; Poli et al. 2020; Eliwa et al. 2021), whereas the AKPG is peralkaline in composition, making this model less applicable. Instead, the fine-grained nature of the Abu Kharif MEs is better explained by crystallization along the margins of a magma chamber during emplacement of the granitic magma in the upper crust (Rodríguez & Castro 2017, 2019). This interpretation is consistent with an autolithic (cognate cumulate) origin (discussed below). Such a process provides a viable alternative to magma mixing for the generation of the MEs, particularly in the absence of clear evidence for coeval mafic magmatism associated with the host granite.

In contrast to MEs in the AKPG with A-type affinity, MEs occur in Variscan I-type granitoids in the Western Carpathians (Petrík & Broska 1989; Broska & Uher 2001), which represent injection of mantle-derived melts into felsic magmas (magma mixing and mingling) (e.g., Broska et al. 2013). Consequently, MEs represent key petrogenetic markers of the interplay between mantle input, crustal melting, and magmatic differentiation during the Variscan orogeny (Hraško et al. 1998; Putiš et al. 2024). Furthermore, Broska et al. (2024b) proposed that the low abundance or even absence of MEs in Western Carpathian I-type granites is related to slab break-off processes and subsequent asthenospheric upwelling. The associated increase in heat flow led to elevated magma temperatures, promoting a complete dissolution of MEs.

Alkaline A-type granitic magmas and their enclaves in the ANS

Microgranular enclaves are widespread in I- and S-type granites but are comparatively rare in alkaline, anorogenic granitoids, a feature that remains poorly understood (e.g., Barbarin 1999). Four principal types of enclaves have been described in alkaline (metaluminous to peralkaline) anorogenic granitic systems, including: (i) xenoliths, (ii) disaggregated or restitic material derived from partially melted source rocks, (iii) cognate cumulates formed by early-crystallized minerals, and (iv) highly evolved (i.e. differentiation of F-rich aqueous fluids) rocks (Bonin 1991; Shellnutt et al. 2010). The Abu Kharif MEs do not correspond to the xenolith or highly evolved fluid-related rocks of Bonin (1991), as evidenced by the absence of F-rich hydrothermal mineral assemblages and other indicators of extensive fluid-mediated alteration.

The scarcity of enclaves in peralkaline A-type granites is commonly attributed to their petrogenesis, which is dominated by extensive fractional crystallization of mantle-derived mafic magmas (Eby 1990, 1992; Shellnutt et al. 2010). Efficient chemical and thermal homogenization during magma evolution generally limits the preservation of discrete enclaves. In contrast, I- and S-type granites commonly involve crustal melting and interaction between compositionally distinct magmas (e.g., Barnes et al. 2021; Eliwa et al. 2021), promoting incomplete homogenization and enclave formation. Nevertheless, magma hybridization is not restricted to I- and S-type granites. Peralkaline A-type granites may also preserve evidence of mafic recharge and magma mixing, expressed by the MEs, disequilibrium mineral assemblages, reverse zoning, and transitional geochemical signatures (Bonin 2007; Frost & Frost 2011). Recent examples include the Krasnopol intrusion, Poland (Domańska-Siuda et al. 2024), and the Hiltaba Suite, Australia (Kontonikas-Charos et al. 2023), demonstrating that enclave formation depends on the dynamics of individual magmatic systems rather than granite type alone. In contrast, the occurrence of xenoliths is largely controlled by mechanical incorporation of country rocks and therefore should not differ significantly among I-, S-, and A-type granitoids.

Accordingly, the geochemical characteristics of the AKPG (Abdel Wanees et al. 2022) indicate a distinct petrogenetic evolution involving partial melting of the juvenile crust of the ANS, followed by extensive fractional crystallization of a peralkaline magma and subsolidus re-equilibration. The relatively unfractionated HREE pattern, coupled with high HREE abundances, is inconsistent with melting in the presence of residual garnet and instead suggests derivation from a garnet-free source (Wilson 2007). The high Rb/Sr ratio (average 4.77) together with elevated Y (average 58.97 ppm) and HREE concentrations are incompatible with melts derived from lower crustal sources. Instead, these geochemical features suggest that the AKPG was generated by partial melting of a metasomatized juvenile Pan-African crust, where infiltration of Na-rich fluids may have promoted crustal anatexis and generated the peralkaline magma (Abdel-Rahman 2006). This interpretation argues against significant mantle–crust magma hybridization during the generation of the AKPG. Flame and vein perthites in the AKPG are interpreted as primary exsolution lamellae formed during slow subsolidus cooling, whereas patch and feather perthites developed through fluid-assisted dissolution–reprecipitation and coarsening of earlier perthitic intergrowths during late-stage hydrothermal alteration (Parsons et al. 2015; Parsons 2021). This interpretation is further supported by the occurrence of titanite replacing amphibole in the Abu Kharif MEs, indicating late-stage fluid-mediated alteration and re-equilibration under oxidizing conditions.

In the ANS, the occurrence of MEs in peralkaline to alkaline granites has been attributed either to bimodal magmatism derived from a common source (Mushkin et al. 2003; Chazot & Bertrand 1995) or to liquid immiscibility within a single magma (El-Dokouny et al. 2023). The coexistence of co-magmatic mafic and felsic rocks of A-type affinity is well documented in the ANS. Such associations are commonly interpreted as resulting from extensive fractional crystallization of mantle-derived mafic magma (often exceeding 90 % crystallization) to produce felsic derivatives, with variable degrees of crustal assimilation during the emplacement, as exemplified by the Amram magmatic suite at the northernmost part of the ANS (Mushkin et al. 2003). However, this scenario is incompatible with the Abu Kharif MEs. These enclaves are dominated by mafic minerals, comprising more than 50 vol. % of the mode, which is inconsistent with their derivation as a liquid composition.

Alternatively, mafic enclaves and their felsic host granites may represent conjugate liquids derived from a single parental melt through silicate–fluoride (Ca-rich) liquid immiscibility, as proposed for microgranular enclaves in the fluorite-bearing Gabal El-Ineigi granite, Central Eastern Desert of Egypt (El-Dokouny et al. 2023). In the immiscible liquid model, the host granite and enclaves represent compositionally distinct liquids derived from a common parental magma (e.g., Veksler et al. 2008). Consequently, their mineral assemblages are typically dissimilar and show no compositional overlap (El-Dokouny et al. 2023). Such immiscibility in alkaline system generally requires elevated F contents (>4 wt. %) in the parental magma (e.g., Klemme 2004). However, these features are inconsistent with the AKPG and associated MEs, as the host alkaline granite lacks fluorite and other F-rich minerals, and the mineral assemblages of both the AKPG and MEs are similar, exhibit compositional overlap, and show some degree of chemical evolution (Figs. 5, 7 and 8) but differ only in mineral proportions.

Evidence for autolith origin

The mineral assemblages of the MEs and their host AKPG are broadly similar, with only minor differences in modal proportions (Fig. 5). Both MEs and the host AKPG share common phases, including albite, K-feldspar, Na–Ca amphibole, Mn-rich ilmenite, quartz, and Ti-rich magnetite. However, titanite occurs exclusively in the enclaves, where it commonly replaces amphibole, as indicated by textural relationships and chemical compositions (Fig. 4d). In contrast, Mn-rich ilmenite, titanomagnetite and zircon are more abundant in the host peralkaline granite than in the enclaves, whereas quartz is comparatively less abundant in the enclaves. Overall, the enclaves are characterized by a higher modal proportion of mafic minerals, particularly amphibole (ferro-richterite, katophorite, and ferro-winchite), titanite and Mn-rich ilmenite – which collectively constitute more than 50 vol. % of the mode. This contrasts with the host granites, where felsic minerals, such as albite, quartz and K-feldspar, are dominant. During the earliest crystallization phases of a granitic melt, mafic minerals will nucleate more quickly than felsic minerals and thus should be enriched in the early crystallization products (e.g., Sun et al. 2022). The ellipsoidal shapes of the Abu Kharif MEs and broadly similar mineral assemblages between the enclaves

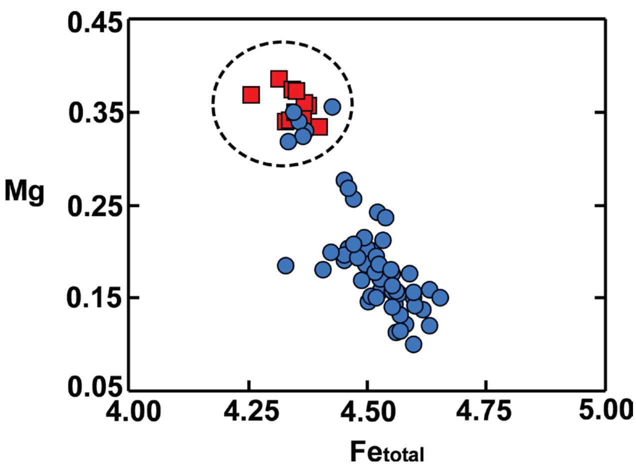

Fig. 7. Binary diagram of Mg (apfu) versus Fe_{total} (apfu) for amphiboles from the host granite and associated enclaves, illustrating the dominant role of fractional crystallization in the evolution of the Abu Kharif peralkaline granitic magma.

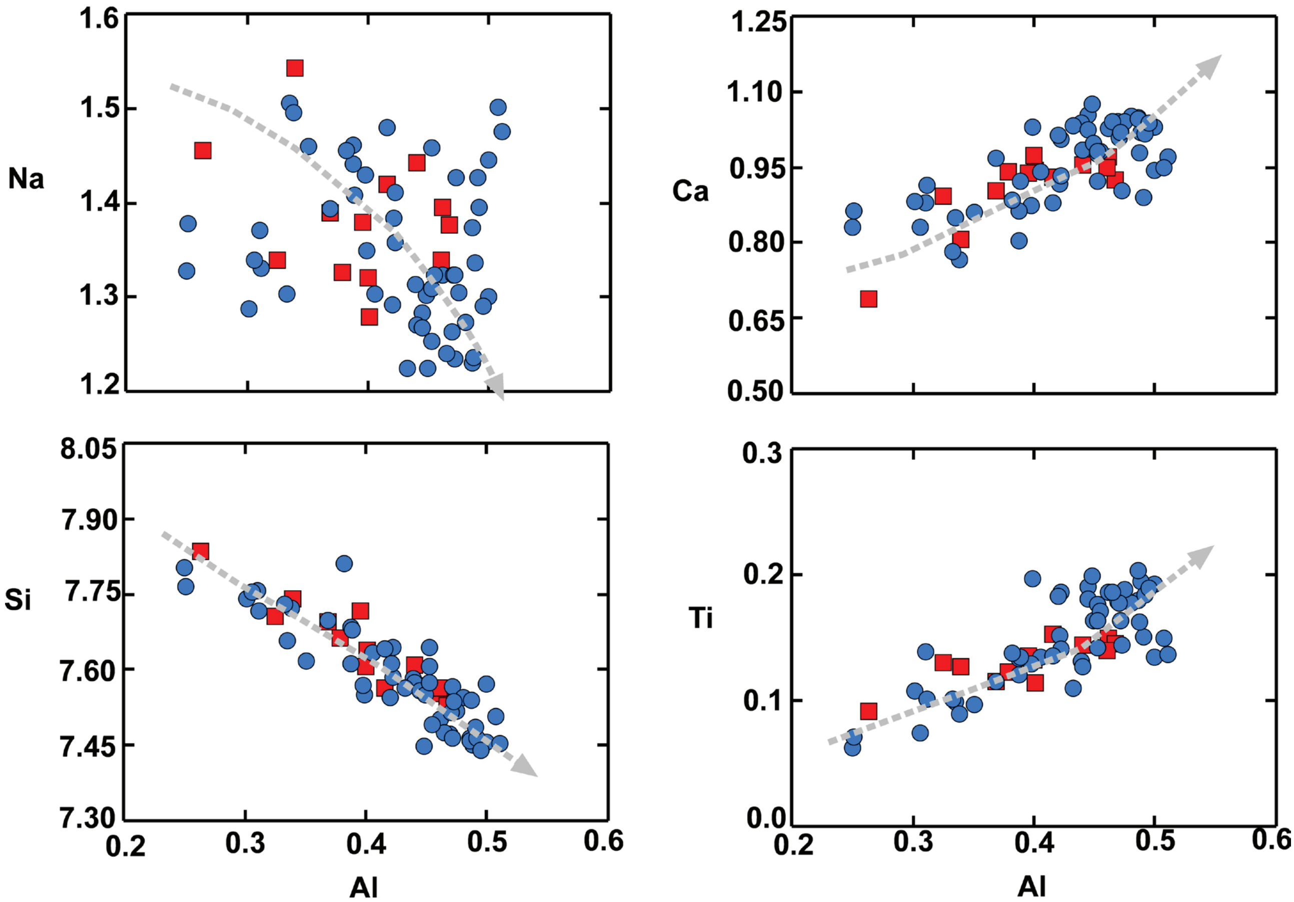

Fig. 8. Binary diagrams of Al (apfu) versus Na, Ca, Si, and Ti (apfu) for amphiboles from the host granite and associated enclaves, illustrating their use as tracers of magmatic differentiation and elemental incompatible behavior.

and their host granites indicate that the enclaves behaved as plastic bodies and remained in thermal equilibrium with the surrounding magma during the emplacement. These features suggest that the enclaves represent accumulations of early-formed mineral phases (i.e., not liquid composition), which is consistent with autolithic origin.

The ferrorichterites and other amphiboles from the Abu Kharif MEs are more magnesian than those of the host AKPG (Fig. 7). This evidence suggests that fractional crystallization was the dominant process within the AKPG granitic magma. Aluminum in the amphibole is used as a key proxy for tracking magmatic differentiation of the host granite, as its concentration in amphibole sensitively records evolving melt conditions, particularly in systems dominated by alkali feldspar fractionation (e.g., Hawthorne et al. 2001; Piilonen et al. 2013). Amphiboles from the AKPG and related MEs define coherent compositional trends, with Al showing positive correlations with Ca and Ti, and inverse correlations with Si and Na (Fig. 8), reflecting systematic crystal-chemical adjustments during the magma evolution. These chemical trends are consistent with magma differentiation, during which Na^+ replaces Ca^{2+} at the B site, while Si^{4+} substitutes for Al^{3+} in the tetrahedral (T) site in the amphibole (Siegel et al. 2017). This coupled exchange, expressed as $^{B}Ca^{2+} + {}^{T}Al^{3+} \rightarrow {}^{B}Na^{+} + {}^{T}Si^{4+}$, reflects a shift toward more evolved, silica-enriched melt compositions. Comparable evolutionary trends – marked by decreasing Ca and increasing Si in amphibole – have been reported from alkaline complexes such as Ilímaussaq (Greenland), Khibiny (Kola Peninsula, Russia), and the Larvik plutonic suite (Oslo Rift, Norway) (Marks et al. 2004; Konopleva et al. 2008; Piilonen et al. 2013).

Furthermore, Ti concentration in amphibole-group minerals from alkaline rocks is commonly used as an indicator of melt evolution due to its incompatible behavior (Siegel et al. 2017). However, in the Abu Kharif alkaline magma, additional controls influence its distribution. Titanium is preferentially partitioned into coexisting mineral phases, particularly during the early or simultaneous crystallization of Mn-rich ilmenite and Ti-rich magnetite from the granitic magma. These Fe–Ti oxides effectively sequester Ti into their crystal lattices, driving amphibole to lower Ti contents, a feature that is characteristic of the host AKPG. Accordingly, amphiboles in both the MEs and the host AKPG display similar well-defined linear trends, indicating a cogenetic origin within a shared magmatic evolution (Fig. 8).

The Abu Kharif enclaves are microgranular and finer-grained than the host granite, and are relatively less evolved, as indicated by their higher proportion of mafic minerals and lower abundance of felsic phases. These features suggest undercooling conditions, likely developed at the contact between hotter magma and cooler country rocks during the emplacement (Donaire et al. 2005). The widespread distribution of the Abu Kharif MEs throughout the AKPG indicates that this process operated at the scale of the magma chamber. The enclaves commonly contain large K-feldspar phenocrysts (Fig. 4a, b), a feature typical of MEs formed by magma mixing and mingling between compositionally contrasting magmas (Eliwa et al. 2021), or by cognate crystal accumulation (Shellnutt et al. 2010; Flood & Shaw 2014). These phenocrysts were most likely incorporated mechanically (Vernon 1984), according to a magma mingling model. Alternatively, the autolith model explains the microgranular texture of enclaves as a result of rapid cooling along magma chamber margins or conduits, promoting the crystallization of ferromagnesian minerals, particularly amphibole (Naney & Swanson 1980; Donaire et al. 2005). Therefore, the frequent presence of large K-feldspar crystals within the Abu Kharif MEs, surrounded by or enclosing other mafic mineral phases, suggests that amphibole and other phases nucleated heterogeneously on these phases. Because K-feldspars nucleate less readily, they tend to develop into relatively large grains (Flood & Shaw 2014), i.e., the magma at the time of quenching already contained crystals (K-feldspars metacrysts of the AKPG) that served as nucleation sites for the quench mineral phases (such as Na–Ca amphiboles in the Abu Kharif MEs).

Conclusions

- The Abu Kharif peralkaline granite (AKPG) hosts microgranular enclaves (MEs), which are finer-grained and relatively less evolved than the host granite, as indicated by their higher proportion of mafic minerals and lower abundance of felsic phases.
- Amphiboles in the host AKPG and MEs are classified as sodic–calcic amphiboles, including ferro-richterite, katophorite, and ferro-winchite. Plagioclase occurs as nearly pure albite, whereas K-feldspar is represented by perthite.
- The mineral assemblages of the AKPG and MEs are broadly similar, exhibit compositional overlaps, and show evidence of chemical evolution, but differ mainly in the relative proportions of their constituent minerals. The MEs contain abundant mafic minerals (>50 vol. % of the modal mineral assemblage), inconsistent with their derivation as a liquid composition.
- Amphiboles from both the MEs and host AKPG display similar, well-defined compositional trends, suggesting a cogenetic relationship and evolution from a common magmatic system. The finer grain size and relatively less evolved character of the MEs compared with the host granite are consistent with undercooling, probably developed at the interface between hotter magma and cooler country rocks during emplacement. These features, together with the mineralogical and compositional similarities between the MEs and host granite, support an autolithic origin for the MEs.

Acknowledgments: The author thanks greatly Prof. Tsuyoshi Iizuka, Dr. Ito Kengo and Koji Ichimura for assistance with the electron microprobe and the staff and technicians of the Department of Earth and Planetary Science, The University of Tokyo. Mineral chemistry, X-ray elemental maps and BSE imaging were supported by EJEP (Egypt–Japan educational partnership; grant 420016 for Nasser M. Mahdy), while field work, logistics, and 4×4 vehicle cars supported by Nuclear Materials Authority of Egypt.

References

Abdel Wanees N.G., El-Sayed M.M., Khalil K.I. & Khamis H.A. 2022: Petrogenesis of contrasting magmatic suites in the Abu Kharif area, Northern Eastern Desert, Egypt: implications for Pan-African crustal evolution and tungsten mineralization. *Geological Magazine* 159, 441–467. https://doi.org/10.1017/S0016756821001047

Abdel-Rahman A.M. 2006: Petrogenesis of anorogenic peralkaline granitic complexes from Eastern Egypt. *Mineralogical Magazine* 70, 27–50. https://doi.org/10.1180/0026461067010311

Barbarin B. 1999: A review of the relationship between granitoid types, their origins and their geodynamic environments. *Lithos* 46, 605–626. https://doi.org/10.1016/S0024-4937(98)00085-1

Barnes C.G., Werts K., Memeti V., Paterson S.R. & Bremer R. 2021: A tale of five enclaves: Mineral perspectives on origins of mafic enclaves in the Tuolumne Intrusive Complex. *Geosphere* 17, 352–374. https://doi.org/10.1130/GES02233.1

Blundy J.D. & Sparks R.S.J. 1992: Petrogenesis of mafic inclusions in granitoids of the Andamello Massif, Italy. *Journal of Petrology* 33, 1039–1053. https://doi.org/10.1093/petrology/33.5.1039

Boehnke P., Watson E.B., Trail D., Harrison T.M. & Schmitt A.K. 2013: Zircon saturation re-revisited. *Chemical Geology* 351, 324–334. https://doi.org/10.1016/j.chemgeo.2013.05.028

Bonin B. 1991: The enclaves of the alkaline anorogenic granites: An overview. In: Didier J. & Barbarin B. (Eds.): *Developments in Petrology 13*. Elsevier, Amsterdam, 179–189.

Bonin B. 2007: A-type granites and related rocks: evolution of a concept, problems and prospects. *Lithos* 97, 1–29. https://doi.org/10.1016/j.lithos.2006.12.007

Broska I. & Uher P. 2001: Whole-rock chemistry and genetic typology of the West-Carpathian Variscan granites. *Geologica Carpathica* 52, 79–90.

Broska I., Petrík I., Be'eri-Shlevin Y. & Majka J. 2013: Devonian/Mississippian I-type granitoids in the Western Carpathians: A subduction-related hybrid magmatism. *Lithos* 162–163, 27–36. https://doi.org/10.1016/j.lithos.2012.12.014

Broska I., Janák M., Svojtka M., Yi K., Konečný P., Kubiš M., Kurylo S., Hrdlička M. & Maraszewska M. 2022: Variscan granitic magmatism in the Western Carpathians with linkage to slab break-off. *Lithos* 412–413, 106589. https://doi.org/10.1016/j.lithos.2021.106589

Broska I., Petrik I., Yi K., Majka J., Barnes C.J., Vojtko R., Madaras J., Kurylo S. & Kubiš M. 2024a: Alpine stacking of two Variscan granite blocks recognised from mineral stabilities, age and structural data (Western Carpathians). *Chemical Geology* 648, 121959. https://doi.org/10.1016/j.chemgeo.2024.121959

Broska I., Keewook Y., Kurylo S., Petrík I., Janák M., Maraszewska M. & Ondrejka M. 2024b: Variscan magmatism with linkage to slab-breakoff? Implication from age data and mineralogy in the Western Carpathians granitic rocks. In: *IGC 2024 Abstract Book.* 37th International Geological Congress 2024, Busan, South Korea, 1093.

Chappell B.W. & White A.J.R. 1991: Restite enclaves and the restite model. In: Didier J. & Barbarin B. (Eds.): *Developments in Petrology 13*. Elsevier, Amsterdam, 375–381.

Chazot G. & Bertrand H. 1995: Genesis of silicic magmas during tertiary continental rifting in Yemen. *Lithos* 36, 69–83. https://doi.org/10.1016/0024-4937(95)00012-5

Chen S.E., Fan S., Yang L., Zhang Y., Zhang L., Liu L. & Zhang T. 2018: The characteristics, origin, and significance of mafic microgranular enclaves in the granitoids from the Bailingshan complex, Eastern Tianshan, NW China. *Geological Journal* 53, 87–96. https://doi.org/10.1002/gj.3232

Chen Y.D., Price R.C. & White A.J.R. 1989: Inclusions in three S-type granites from southeastern Australia. *Journal of Petrology* 30, 1181–1218. https://doi.org/10.1093/petrology/30.5.1181

Cox G.M., Lewis C.J., Collins A.S., Halverson G.P., Jourdan F., Foden J., Nettle D. & Kattan F. 2012: Ediacaran terrane accretion within the Arabian-Nubian Shield. *Gondwana Research* 21, 341–352. https://doi.org/10.1016/j.gr.2011.02.011

Dessouky O.K., Li H., Ali H.H., Dardier A.M., Ali K.A., Pirajno F., Saleh G.M., Omran A.A., Hassan I.S., Luo Z. & Hassan M.M. 2024: Ediacaran anorogenic alkaline magmatism and wolframite mineralization linked to mantle plume activity in the north Arabian-Nubian Shield (Egypt). *Geochemistry* 84, 126119. https://doi.org/10.1016/j.chemer.2024.126119

Domańska-Siuda J., Grabarczyk-Gurba A. & Nejbert K. 2024: Petrogenesis of microgranular enclaves in the A-type granitoid Krasnopol intrusion (Mazury Complex, northeastern Poland): Evidence of magma mixing. *Mineralogy and Petrology* 118, 401–426. https://doi.org/10.1007/s00710-024-00866-1

Donaire T., Pascual E., Pin C. & Duthou J.L. 2005: Microgranular enclaves as evidence of rapid cooling in granitoid rocks: The case of the Los Pedroches granodiorite, Iberian Massif, Spain. *Contributions to Mineralogy and Petrology* 149, 247–265. https://doi.org/10.1007/s00410-005-0652-0

Eby G.N. 1990: The A-type granitoids: A review of their occurrence and chemical characteristics and speculations on their petrogenesis. *Lithos* 26, 115–134. https://doi.org/10.1016/0024-4937(90)90043-Z

Eby G.N. 1992: Chemical subdivision of the A-type granitoids: Petrogenetic and tectonic implications. *Geology* 20, 641–644. https://doi.org/10.1130/0091-7613(1992)020

El-Bialy M.Z., Eliwa H.A., Mahdy N.M., Murata M., El-Gameel K.H., Sehsah H., Omar M., Kato Y., Fujinaga K., Andresen A. & Thomsen T.B. 2020: U–Pb zircon geochronology and geochemical constraints on the Ediacaran continental arc and post-collision granites of Wadi Hawashiya, North Eastern Desert, Egypt. *Precambrian Research* 345, 105777. https://doi.org/10.1016/j.precamres.2020.105777

El-Dokouny H.A., Mahdy N.M., El Hadek H.H., Sami M., Abart R., Ahmed M.S., Zafar T. & Sanislav I.V. 2023: Origin of amphibole–biotite–fluorite-rich enclaves from Gabal El-Ineigi fluorite-bearing granite, central Eastern Desert of Egypt: Insights into fluoride–calcium and silicate liquid immiscibility. *Minerals* 13, 670. https://doi.org/10.3390/min13050670

El-Sayed M.M. 1998: Tectonic setting and petrogenesis of the Kadabora pluton: A late Proterozoic anorogenic A-type younger granitoid in the Egyptian Shield. *Chemie der Erde* 58, 38–63.

El-Shazly A.K. & Khalil K.I. 2016: Metamorphic and geochronologic constraints on the tectonic evolution of the Central Eastern Desert of Egypt. *Precambrian Research* 283, 144–168. https://doi.org/10.1016/j.precamres.2016.07.016

Eliwa H.A., Deevsalar R., Mahdy N.M., Kumar S., El-Gameel Kh., Zafar T., Khalaf I.M., Murata M., Ozawa H., Andresen A., Chew D., Fawzy M.M., Afandy A., Kato Y. & Fujinaga K. 2021: Field, textural, geochemical, and isotopic constraints on the origin and evolution of the magmatic microgranular enclaves from the Gharib Granitoid Complex, North Eastern Desert, Egypt. *Precambrian Research* 365, 106380. https://doi.org/10.1016/j.precamres.2021.106380

Flood R.H. & Shaw S.E. 2014: Microgranitoid enclaves in the felsic Looanga monzogranite, New England Batholith, Australia: Pressure quench cumulates. *Lithos* 198, 92–102. https://doi.org/10.1016/j.lithos.2014.03.015

Fréville K., Jacob J.B., Vanardois J., Trap P., Melleton J., Faure M., Guillot S., Janots E., Bruguier O., Poujol M. & Lach P. 2024: Protracted magmatism and crust–mantle interaction during continental collision: insights from the Variscan granitoids of the external western Alps. *International Journal of Earth Sciences* 113, 1165–1196. https://doi.org/10.1007/s00531-024-02420-y

Frost C.D. & Frost B.R. 2011: On ferroan (A-type) granitoids: their compositional variability and modes of origin. *Journal of Petrology* 52, 39–53. https://doi.org/10.1093/petrology/egq070

Gómez-Frutos D. & Castro A. 2023: Mafic microgranular enclaves (MMEs) trace the origin of post-collisional magmas. *Geology* 51, 743–747. https://doi.org/10.1130/G51248.1

Hawthorne F.C., Oberti R., Cannillo E., Ottolini L., Roelofsen J.N. & Martin R.F. 2001: Li-bearing arfvedsonitic amphiboles from the Strange Lake peralkaline granite, Quebec. *Canadian Mineralogist* 39, 1161–1170. https://doi.org/10.2113/gscanmin.39.4.1161

Hawthorne F.C., Oberti R., Harlow G.E., Maresch W.V., Martin R.F., Schumacher J.C. & Welch M.D. 2012: Nomenclature of the amphibole supergroup. *American Mineralogist* 97, 2031–2048. https://doi.org/10.2138/am.2012.4276

Hraško Ľ., Kotov A.B., Salnikova E.B. & Kovach V.P. 1998: Enclaves in the Rochovce granite intrusion as indicators of the temperature and origin of the magma. *Geologica Carpathica* 49, 125–138.

Jacobs J. & Thomas R.J. 2004: Himalayan-type indenter-escape tectonics model for the southern part of the late Neoproterozoic–early Paleozoic East African Antarctic orogen. *Geology* 32, 721–724. https://doi.org/10.1130/G20516.1

King P.L., Sham T.K., Gordon R.A. & Dyar M.D. 2013: Microbeam X-ray analysis of Ce^{3+}/Ce^{4+} in Ti-rich minerals: A case study with titanite (sphene) with implications for multivalent trace element substitution in minerals. *American Mineralogist* 98, 110–119. https://doi.org/10.2138/am.2013.3959

Klemme S. 2004: Evidence for fluoride melts in Earth's mantle formed by liquid immiscibility. *Geology* 32, 441–444. https://doi.org/10.1130/G20328.1

Kohút M. & Larionov A.N. 2021: From subduction to collision: Genesis of the Variscan granitic rocks from the Tatric Superunit (Western Carpathians, Slovakia). *Geologica Carpathica* 72, 96–113. https://doi.org/10.31577/GeolCarp.72.2.2

Kohút M., Stein H.J., Chovan M., Majzlan J. & Ozdin D. 2024: Duration of Variscan granitic magmatism inferred from Re–Os dating of molybdenite in the Tatric Unit of the Western Carpathians. *Geologica Carpathica* 75, 303–313. https://doi.org/10.31577/GeolCarp.2024.17

Konopleva N.G., Ivanyuk G.Y., Pakhomovsky Y.A., Yakovenchuk V.N., Menshikov Y.P. & Korchak Y.A. 2008: Amphiboles of the Khibiny alkaline pluton, Kola Peninsula, Russia. *Geology of Ore Deposits* 50, 720–731. https://doi.org/10.1134/S1075701508080084

Kontonikas-Charos A., Ehrig K., Cook N.J. & Ciobanu C.L. 2023: Mafic mineral clots and microgranular enclaves in A-type Hiltaba Suite granites from the Gawler Craton, South Australia: Origins and implications. *Lithos* 446, 107114. https://doi.org/10.1016/j.lithos.2023.107114

Kowallis B.J., Christiansen E.H., Dorais M.J., Winkel A., Henze P., Franzen L. & Mosher H. 2022: Variation of Fe, Al and F substitution in titanite (sphene). *Geosciences* 12, 229. https://doi.org/10.3390/geosciences12060229

Kröner A., Kruger J. & Rashwan A.A. 1994: Age and tectonic setting of granitoid gneisses in the Eastern Desert of Egypt and southwest Sinai. *Geologische Rundschau* 83, 502–513. https://doi.org/10.1007/BF01083223

Kumar S. & Pieru T. 2010: Petrography and major elements geochemistry of microgranular enclaves and Neoproterozoic granitoids of South Khasi, Meghalaya: Evidence of magma mixing and alkali diffusion. *Journal of the Geological Society of India* 76, 345–360. https://doi.org/10.1007/s12594-010-0106-9

Kumar S. & Rino V. 2006: Mineralogy and geochemistry of microgranular enclaves in Palaeoproterozoic Malanjkhand granitoids, central India: evidence of magma mixing, mingling, and chemical equilibration. *Contributions to Mineralogy and Petrology* 152, 591–609. https://doi.org/10.1007/s00410-006-0122-3

Kumar S., Rino V. & Pal A.B. 2004: Field evidence of magma mixing from microgranular enclaves hosted in Early Proterozoic Malanjkhand granitoids, central India. *Gondwana Research* 7, 539–548. https://doi.org/10.1016/S1342-937X(05)70804-2

Leake B.E., Woolley A.R., Arps C.E., Birch W.D., Gilbert M.C., Grice J.D., Hawthorne F.C., Kato A., Kisch H.J., Krivovichev V.G. & Linthout K. 1997: Nomenclature of amphiboles: Report of the subcommittee on amphiboles of the International Mineralogical Association. *Canadian Mineralogist* 35, 219–246.

Liégeois J.P. & Black R. 1987: Alkaline magmatism subsequent to collision in the Pan-African belt of the Adrar des Iforas (Mali). *Geological Society, London, Special Publications* 30, 381–401. https://doi.org/10.1144/GSL.SP.1987.030.01.18

Mahdy N.M. 2026: Mineral texture and chemistry of plagioclase, biotite, and titanite from the Abu Kharif biotite granite, Northern Eastern Desert, Egypt: Constraints on the genesis of I-type granite-related tungsten mineralization. *Journal of African Earth Sciences* 242, 106244. https://doi.org/10.1016/j.jafrearsci.2026.106244

Mahdy N.M., El-Arafy R.A., El-Qassas R.A., Metwaly M., Abd El-Rahman Y., El-Sundolly H.I. & Said A. 2024: Lithological discrimination of the Fawakhir-Atalla belt in the Central Eastern Desert of Egypt. *Physics and Chemistry of the Earth* 134, 103578. https://doi.org/10.1016/j.pce.2024.103578

Mandl M., Kurz W., Hauzenberger C., Fritz H. & Pfingstl S. 2022: Geochemistry of granitoids from the Austroalpine Seckau Complex: A key for revealing the pre-Alpine evolution of the Eastern Alps. *Mineralogy and Petrology.* 116, 251–272. https://doi.org/10.1007/s00710-022-00781-3

Marks M., Halama R., Wenzel T. & Markl G. 2004: Trace element variations in clinopyroxene and amphibole from alkaline to peralkaline syenites and granites. *Chemical Geology* 211, 185–215. https://doi.org/10.1016/j.chemgeo.2004.06.032

Marks M.A. & Markl G. 2017: A global review on agpaitic rocks. *Earth-Science Reviews* 173, 229–258. https://doi.org/10.1016/j.earscirev.2017.06.002

Mitchell R.H. & Liferovich R.P. 2004: Ecandrewsite-zincian pyrophanite from lujavrite, Pilansberg alkaline complex, South Africa. *Canadian Mineralogist* 42, 1169–1178. https://doi.org/10.2113/gscanmin.42.4.1169

Mushkin A., Navon O., Halicz L., Hartmann G. & Stein M. 2003: The petrogenesis of A-type magmas from the Amram Massif, southern Israel. *Journal of Petrology* 44, 815–832. https://doi.org/10.1093/petrology/44.5.815

Naney M.T. & Swanson S.E. 1980: The effect of Fe and Mg on crystallization in granitic systems. *American Mineralogist* 65, 639–653.

Parsons I. 2021: Feldspars. In: Alderton D. & Elias S.A. (Eds.): *Encyclopedia of Geology*. Second Edition, Academic Press, London, 271–286. https://doi.org/10.1016/B978-0-12-409548-9.12101-3

Parsons I., Fitz Gerald J.D. & Lee M.R. 2015: Routine characterization and interpretation of complex alkali feldspar intergrowths. *American Mineralogist* 100, 1277–1303. https://doi.org/10.2138/am-2015-5094

Perugini D., Ventura G., Petrelli M. & Poli G. 2004: Kinematic significance of morphological structures generated by mixing of magmas: A case study from Salina Island (southern Italy). *Earth and Planetary Science Letters* 222, 1051–1066. https://doi.org/10.1016/j.epsl.2004.03.038

Perumalsamy C., Vijay Anand S., Nagarajan R. & Mukherjee B. 2024: Petrogenesis of S-type Ladakh granite and mafic microgranular enclaves in the southern margin of Ladakh batholith: An evidence of crust–mantle interaction during the collision between Indian and Eurasian plates. *Island Arc* 33, e12520. https://doi.org/10.1111/iar.12520

Petrík I. & Broska I. 1989: Mafic enclaves in granitoid rocks of the Tribeč Mountains, Western Carpathians: Geochemistry and petrology. *Geologický Zborník* 40, 667–695.

Petrík I. & Broska I. 1994: Petrology of two granite types from the Tribeč Mountains, Western Carpathians: an example of allanite (+ magnetite) versus monazite dichotomy. *Geological Journal* 29, 59–78. https://doi.org/10.1002/gj.3350290106

Piilonen P.C., McDonald A.M., Poirier G., Rowe R. & Larsen A.O. 2013: Mafic minerals of the alkaline pegmatites in the Larvik Plutonic Complex, Oslo Rift, Southern Norway. *Canadian Mineralogist* 51, 735–770. https://doi.org/10.3749/canmin.51.5.735

Poli G., Christofides G., Koroneos A., Trajanova M. & Zupančič N. 2020: Multiple processes in the genesis of the Pohorje igneous complex. *Lithos* 364–365, 105512. https://doi.org/10.1016/j.lithos.2020.105512

Putiš M., Ondrejka M., Nemec O., Li Q., Chew D., Li X.H., Madarás J., Németh Z., Spišiak J., Siman P. & Ružička P. 2024: The Western Carpathians Variscan orogen: A collage of post-Cadomian, Cenerian, and Paleotethyan complexes from Gondwana-derived terranes (a new concept). In: *Environmental, Structural and Stratigraphical Evolution of the Western Carpathians, Abstract book*. Comenius University Bratislava, 57–61. https://geopaleo.sk/wp-content/uploads/2025/01/Esseweca-2024.pdf

Rodríguez C. & Castro A. 2017: Silicic magma differentiation in ascent conduits. *Lithos* 272–273, 261–277. https://doi.org/10.1016/j.lithos.2016.12.017

Rodríguez C. & Castro A. 2019: Origins of microgranular enclaves and enclave swarms in granites. *Geological Society of America Bulletin* 131, 635–660. https://doi.org/10.1130/B32028.1

Salvi S. & Williams-Jones A.E. 2022: Alkaline and peralkaline igneous rocks and rare metals. *Elements* 18, 331–336. https://doi.org/10.2138/gselements.18.5.331

Schönenberger J., Marks M., Wagner T. & Markl G. 2006: Fluid-rock interaction in autoliths of agpaitic nepheline syenites in the Ilímaussaq intrusion, South Greenland. *Lithos* 91, 331–351. https://doi.org/10.1016/j.lithos.2006.03.024

Shellnutt J.G., Jahn B.M. & Dostal J. 2010: Elemental and Sr–Nd isotope geochemistry of microgranular enclaves. *Lithos* 119, 34–46. https://doi.org/10.1016/j.lithos.2010.07.011

Siegel K., Williams-Jones A.E. & van Hinsberg V.J. 2017: The amphiboles of the REE-rich A-type peralkaline Strange Lake pluton. *Lithos* 288, 156–174. https://doi.org/10.1016/j.lithos.2017.07.012

Spišiak J., Kohút M., Butek J., Ferenc Š., Šimonová V., Kopáčik R. & Chew D. 2024: Petrology, geochronology, and origin of gabbrodioritoid rocks from Veľké Železné (Nízke Tatry Mts., Western Carpathians, Slovakia). *Geologica Carpathica* 75, 3–20. https://doi.org/10.31577/GeolCarp.2024.02

Stampfli G.M. and Borel G.D. 2002: A plate tectonic model for the Paleozoic and Mesozoic constrained by dynamic plate boundaries and restored synthetic oceanic isochrons. *Earth and Planetary Science Letters* 196, 17–33. https://doi.org/10.1016/S0012-821X(01)00588-X

Stern R.J. 1994: Neoproterozoic arc assembly and continental collision in the East African Orogen. *Annual Review of Earth and Planetary Sciences* 22, 319–351. https://doi.org/10.1146/annurev.ea.22.050194.001535

Stern R.J. 2018: Neoproterozoic formation and evolution of Eastern Desert continental crust: The importance of the infrastructure–superstructure transition. *Journal of African Earth Sciences* 18, 15–27. https://doi.org/10.1016/j.jafrearsci.2017.01.001

Sun Z., Dong G., Ketchaya Y.B., Pan Y., Wang W., Xu L., Guo J., Wang Z. & Fu B. 2022: Petrogenesis of microgranitoid enclaves and their host granites. *Geological Journal* 57, 208–220. https://doi.org/10.1002/gj.4292

Veksler I.V., Dorfman A.M., Rhede D., Wirth R., Borisov A.A. & Dingwell D.B. 2008: Liquid unmixing kinetics and the extent of immiscibility in the system K_2O–CaO–FeO–Al_2O_3–SiO_2. *Chemical Geology* 256, 119–130. https://doi.org/10.1016/j.chemgeo.2008.06.033

Vernon R.H. 1983: Restite, xenoliths and microgranitoid enclaves in granites. *Journal & Proceedings, Royal Society of New South Wales* 116, 77–109.

Vernon R.H. 1984: Microgranitoid enclaves in granites: Globules of hybrid magma quenched in a plutonic environment. *Nature* 309, 438–439. https://doi.org/10.1038/309438a0

Vernon R.H. 2010: Granites really are magmatic: Using microstructural evidence to refute some hypotheses. *Journal of the Virtual Explorer* 35, 3. https://doi.org/10.3809/jvirtex.2011.00264

White A.J.R., Chappell B.W. & Wyborn D. 1999: Application of the restite model to the Deddick Granodiorite and its enclaves. *Journal of Petrology* 40, 413–421. https://doi.org/10.1093/petroj/40.3.413

Wilson M. 2007: Relation of present-day magmatism to global tectonic processes. In: I*gneous Petrogenesis*. Springer Netherlands, Dordrecht, 3–12. https://doi.org/10.1007/978-94-010-9388-0_1

Wu T., Zhang W. & Wilde S.A. 2020: The origin of mafic microgra_ nular enclaves in granitoids: Insights from in situ Sr isotope of plagioclases and Zr–Hf isotopes of zircons. *Chemical Geology* 551, 119776. https://doi.org/10.1016/j.chemgeo.2020.119776

Zafar T., Rehman H.U., Mahar M.A., Alam M., Oyebamiji A., Rehman S.U. & Leng C.B. 2020: A critical review on petrogenetic, metallogenic and geodynamic implications of granitic rocks exposed in north and east China: New insights from apatite geochemistry. *Journal of Geodynamics* 136, 101723. https://doi.org/10.1016/j.jog.2020.101723

Electronic supplementary material is available online:
Supplementary Table S1 at https://geologicacarpathica.com/data/files/supplements/GC77-5-Mahdy_TableS1.xlsx
Supplementary Table S2 at https://geologicacarpathica.com/data/files/supplements/GC77-5-Mahdy_TableS2.xlsx
Supplementary Table S3 at https://geologicacarpathica.com/data/files/supplements/GC77-5-Mahdy_TableS3.xlsx
Supplementary Table S4 at https://geologicacarpathica.com/data/files/supplements/GC77-5-Mahdy_TableS4.xlsx
Supplementary Table S5 at https://geologicacarpathica.com/data/files/supplements/GC77-5-Mahdy_TableS5.xlsx
Supplementary Table S6 at https://geologicacarpathica.com/data/files/supplements/GC77-5-Mahdy_TableS6.xlsx